Adsorption of Argon on Carbon Nanotube Bundles and its Influence on the Bundle Lattice Parameter

M. Bienfait,[1] P. Zeppenfeld,[2,*] N. Dupont-Pavlovsky,[3] J.-P. Palmari,[1] M. R. Johnson,[4] T. Wilson,[5] M. DePies,[5] and O. E. Vilches[5]

[1]*CRMC2-CNRS, Faculté de Luminy, Case 901, F-13288 Marseille CEDEX 9, France*
[2]*Institut für Experimentalphysik, Johannes Kepler Universität Linz, A-4040 Linz, Austria*
[3]*LCSM, Université H. Poincaré, BP 239, F-54506 Vandoeuvre les Nancy CEDEX, France*
[4]*Institut Laue-Langevin, BP 156, F-38042 Grenoble CEDEX 9, France*
[5]*Department of Physics 351560, University of Washington, Seattle, Washington 98195-1560, USA*

(Received 28 February 2003; published 18 July 2003)

We report experimental studies of the adsorption characteristics and structure of both ^{36}Ar and ^{40}Ar on single-wall carbon nanotube bundles. The structural studies make use of the large difference in coherent neutron scattering cross section for the two Ar isotopes to explore the influence of the adsorbate on the nanotube lattice parameter. We observe no dilation of the nanotube lattice with ^{40}Ar, and explain the apparent expansion of this lattice upon ^{36}Ar adsorption by the location of the adsorbed Ar atoms on the outer bundle surface.

DOI: 10.1103/PhysRevLett.91.035503 PACS numbers: 61.48.+c, 61.12.Ld, 68.43.Fg, 68.47.–b

Much attention has been focused recently on the exciting possibilities for one-dimensional (1D) and two-dimensional (2D) adsorption of gases on bundles of single-wall carbon nanotubes (SWNTB) [1–8]. Moreover, the total storage capacity at a given temperature and pressure together with a detailed knowledge on the various available adsorption sites is relevant for potential applications of carbon nanotubes for gas storage, such as for hydrogen used in fuel cells [9]. Carbon nanotubes are made of graphene sheets wrapped around themselves into tubes with a diameter of 1–2 nm and a length of a few μm. For our study and in this Letter, we consider only tubes that are capped at both ends and are hexagonally packed in bundles with a typical diameter of about 10 nm.

SWNTBs exhibit linear arrays of adsorption sites, thus providing a physical realization of 1D matter. The 1D adsorption sites are located in the interstitial channels between the tubes within a bundle and in the grooves separating two adjacent tubes on the outer surface of a bundle. In addition, 2D-like sites are located on the graphene outer surface. Recent calculations [10] predict that rare gas atoms such as Ar can enter the interstitial channels separating perfect monodisperse nanotubes and slightly dilate the bundle lattice by about 0.33 Å, i.e., by about 2% of the 17 Å average distance between adjacent nanotubes. In fact, such a coherent bundle dilation and the concomitant filling of all interstitial sites could result in an increased capacity to store gases in these bundles. An apparent bundle dilation induced upon physisorption has, indeed, been reported for O_2 and N_2 [5] and CD_4 [3], but there is little evidence as to the structure of the adsorbates and bundles themselves, for these or other species.

The aim of this Letter is to understand the adsorption scenario which is still under debate [6–8,10]. In particular, we wanted to explore whether an apparent bundle dilation can be observed during adsorption of Ar on SWNTBs and whether a shift of the diffraction peak associated with the bundle structure is an unambiguous indication for Ar adsorption in the interstitial channels. To this end, we performed contrast neutron diffraction experiments for different quantities of ^{36}Ar and ^{40}Ar deposited on SWNTBs using beam lines D1B and D20 at the ILL-Grenoble. ^{40}Ar has a very small scattering cross section (0.421 barn) and should not modify the carbon nanotube pattern except if it enters into the interstitial channels and expands the lattice in the bundle section. On the other hand, the very large coherent scattering cross section of ^{36}Ar (77.9 barn) should give detailed information on the adsorbate structure.

Our adsorption cells were made of aluminum (neutron diffraction) and glass (adsorption isotherms) containing a powder of SWNTB provided by the GDPC Laboratory of the University of Montpellier [11,12]. The nanotubes were prepared by a yttrium-nickel catalyzed electric arc discharge in a helium atmosphere. This method produces nanotubes closed at both ends. Amorphous and graphitized carbon and metal particles embedded in carbon are present in the sample and easily detectable in the neutron diffraction spectra. A few nanotubes are isolated, but most are associated in bundles involving 30 to 50 individual tubes parallel to each other in a hexagonal arrangement. The distance between two adjacent tubes in a bundle is 17 Å on average, with a slight dispersion of the tube diameters of the order of ± 1 Å [12,13]. This dispersion likely produces a distribution in width and shape of the interstitial channels, as indicated schematically in Fig. 1.

To prepare for and complement the neutron diffraction experiment, we have recorded Ar adsorption isotherms at 77.4, 84.8, and 96.1 K on a fraction (46 mg) of the same

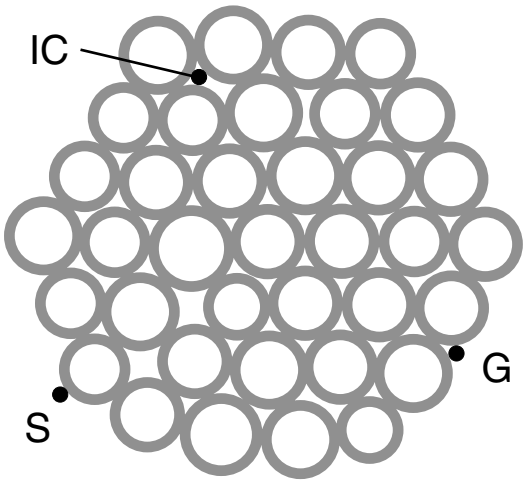

FIG. 1. Schematic section of a nanotube bundle containing 37 nanotubes with a diameter of (17 ± 1) Å. The dispersion of the nanotube diameter gives rise to an imperfect lateral ordering and heterogeneous interstitial channels (IC) providing possible adsorption sites for atoms and small molecules (black dots drawn to the size of a particle with 4 Å diameter). Other adsorption sites are the grooves (G) and the rounded outer surface of the bundle (S).

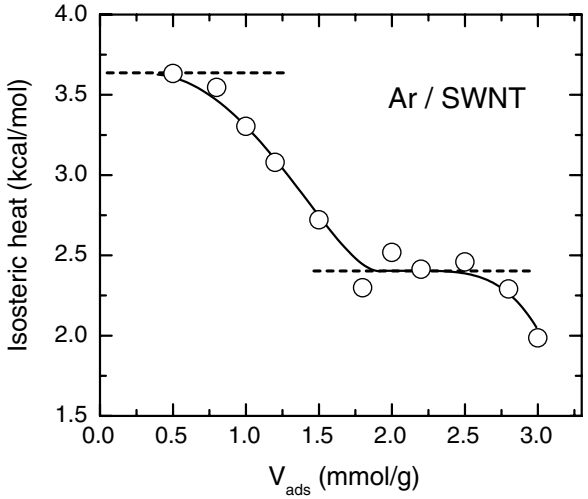

FIG. 2. Isoteric heat of adsorption for Ar adsorbed on single-wall carbon nanotube bundles. The high binding energy sites (3.6 kcal/mol or 156 meV/atom) correspond to the adsorption in the grooves (G) and in the largest interstitial channels (IC), whereas the low energy binding sites (2.4 kcal/mol or 104 meV/atom) correspond to the adsorption, at higher coverages, on the rounded part of the outer graphene surface of the bundles (S).

SWNTB sample. The isotherms (adsorbed volume V_{ads} vs Ar pressure p) show two risers and are similar to those recorded from other small diameter molecules or atoms such as H_2 [4], Kr and CH_4 [2], Xe [6,7], and Ar [4,7]. The lower pressure riser corresponds to an initial adsorption on high binding energy sites, while the higher pressure riser corresponds to graphitelike adsorption on the exterior surfaces of the bundles. From these isotherms, the isosteric heat of adsorption $q_{st}/k_B = -d(\ln p)/d(1/T)$ has been determined in the usual way and the results are shown in Fig. 2.

The diffraction experiments were performed on the 660 mg SWNTB sample used previously for neutron diffraction measurements on CD_4 and D_2 [3]. The sample was outgassed at 150 °C for one day prior to the experiments. Three Ar doses V_{ads} were investigated, corresponding to 0.34, 0.68, and 2.7 mmol/g (see Fig. 2). Ar was slowly introduced into the sample cell at 100 K for the smallest coverages, and at 70 K for the largest. The temperature was then slowly decreased to 40 K. The recording of the neutron diffraction patterns was started when equilibrium was reached—typically after 1 h—and the total measuring time was 10 h per coverage. Most of the experiments were performed on the D20 diffractometer at the Institut Laue-Langevin (ILL) in Grenoble, using a wavelength $\lambda = 2.414$ Å and a scattering vector range $0.2\ \text{Å}^{-1} < Q < 5\ \text{Å}^{-1}$. A few experiments were performed on the D1B diffractometer at ILL, with $\lambda = 2.527$ Å. The results obtained on both instruments were similar and reproducible, with higher quality data obtained on D20.

Neutron diffraction spectra recorded from the bare SWNTB sample and after adsorption of 2.7 mmol/g of ^{36}Ar are shown in Fig. 3(a). These patterns reveal the diffraction lines of the SWNTB, the cell, the cryostat, and the change induced upon adsorption. The features at wave vector transfer $Q = 0.42$, 0.73, 0.85, and 1.1 Å^{-1} result from the hexagonal medium range order of the tubes within the bundles with a periodicity of about 17 Å (see Fig. 1) and correspond to the (10), (11), (20), and (21) Bragg reflections from the bundle lattice, respectively [dotted lines in Fig. 3(a)]. Some of the structures at about 3 Å^{-1} arise from the long range order along the nanotubes in the bundles [12]. In addition, many extra peaks are due to impurities in the substrate, e.g., those between 1.8 and 1.9 Å^{-1} from graphitized carbon, those at 3.1 and 3.6 Å^{-1} from Ni, at 2.7 and 3.1 Å^{-1} from the aluminum container, and the 4.45 Å^{-1} line from Al_2O_3. The diffraction pattern changes upon adsorption of ^{36}Ar. The most significant modification is observed for the 2.7 mmol/g uptake, i.e., for a coverage where almost all adsorption sites are occupied. The changes upon adsorption are most evident in the difference spectrum (^{36}Ar on bundles minus bare bundles) shown in Fig. 3(b). A drop of the intensity is observed between 0.5 and 1.2 Å^{-1} and two broad peaks can be seen, one between 1.5 and 2.4 Å^{-1} and the other between 3 and 4.5 Å^{-1}. The drop arises from a cross interference either between the nanotubes and the atoms or molecules adsorbed in the interstitial channels as already outlined in Ref. [5] or between the nanotubes and the adsorbed species on the outer surface of the

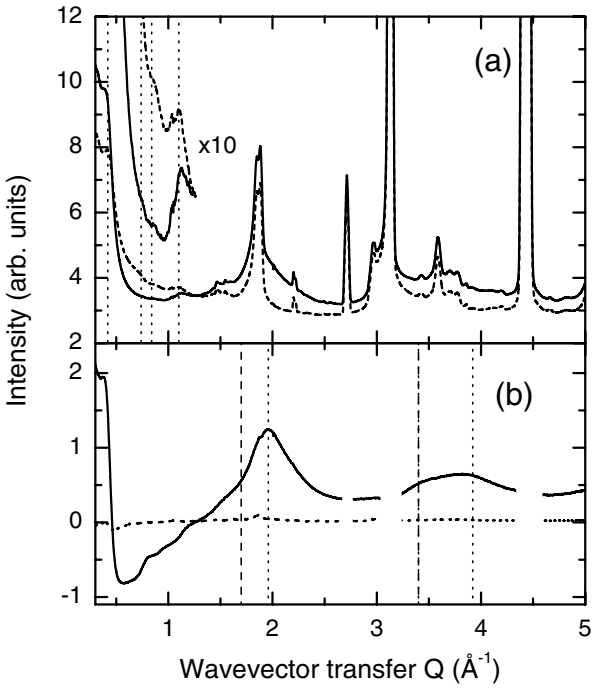

FIG. 3. (a) Neutron diffraction spectra of the bare SWNTB sample (broken line) and upon adsorption of 2.7 mmol/g (solid line) of ^{36}Ar. Vertical dotted lines: Positions of the Bragg peaks expected for a hexagonal packing of nanotubes with a lattice spacing of 17 Å. (b) Solid trace: Difference between the diffraction spectra in (a), revealing the changes induced upon adsorption. Dotted trace: Same but for adsorption of 2.7 mmol/g of ^{40}Ar. Vertical dashed and dotted lines indicate expected Ar peak positions (see text).

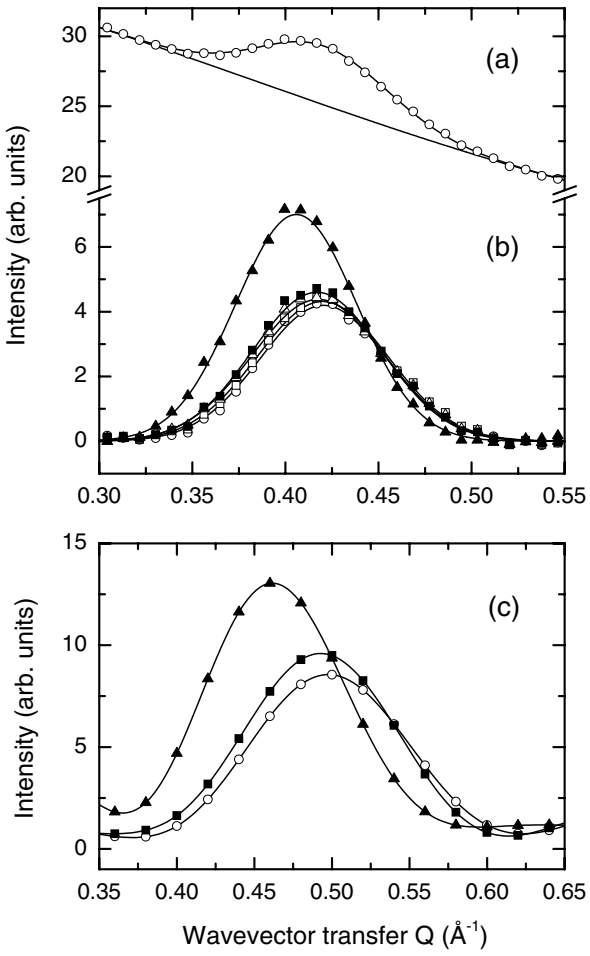

FIG. 4. (a) Neutron diffraction spectrum of the bare SWNTB sample in the vicinity of the (10) bundle lattice peak fitted by the sum of a polynomial of order three (background) and a Gaussian peak (solid lines). (b) Diffraction spectra (after background removal) of the bare SWNTB sample (open circles) and after adsorption of 0.68 and 2.7 mmol/g (squares and upper triangles, respectively) of ^{36}Ar (filled symbols) and ^{40}Ar (open symbols). The solid lines are Gaussian fits to the data. (c) (10) diffraction peak obtained from a simulation of a bare seven (10,10)-SWNT bundle (open circles) and after ^{36}Ar adsorption. The two ^{36}Ar coverages correspond to the filling of the grooves (solid squares) and the complete coverage of the outer surface layer (solid triangles) and can thus be compared to the spectra (same symbols) in (b). Solid lines are guides to the eye.

bundle (groove sites and graphene surface) as shown in recent simulations [14].

The two broad features centered around 2 and 3.8 Å^{-1} comprise a combination of Bragg peaks, arising from small linear patches adsorbed in the grooves plus available interstitial channels and from small two-dimensional islands and narrow strips condensed on the rounded external bundle surface (at higher Ar coverages). The peak positions expected for the Ar nearest neighbor spacing of 3.7 Å in a linear arrangement and in a two-dimensional hexagonal array are indicated by the dashed and dotted lines in Fig. 3(b), respectively. A detailed peak shape analysis will be presented in a forthcoming paper [13].

In the following, we focus on the 0.42 Å^{-1} peak resulting from the medium range order of the nanotubes within the bundles. For a quantitative analysis, the diffraction spectra were fitted by the sum of a polynomial [describing the steep background in Fig. 3(a)] and a Gaussian peak, as illustrated in Fig. 4(a) for the bare SWNTB spectrum. The diffraction peaks after background removal for the two largest ^{36}Ar doses and for the bare SWNTB sample are presented in Fig. 4(b). The peak corresponding to the smaller dose (0.68 mmol/g) exhibits a slight intensity increase and a tiny shift of about (0.003 ± 0.001) Å^{-1}, the error being derived from the statistical uncertainty of the fitted peak positions. The changes are even smaller for the lowest coverage (0.34 mmol/g). However, the diffraction peak obtained for the largest coverage (2.7 mmol/g) exhibits an important intensity increase and a significant shift of the peak maximum by about 0.015 Å^{-1} towards smaller scattering vectors. This corresponds to an increase of the "effective" lattice parameter of about 3%. To check whether this increase

is actually due to an average bundle dilation upon Ar adsorption, we performed neutron diffraction with ^{40}Ar for the same doses.

The neutron cross section of this argon isotope being very small, no change of the SWNT diffraction pattern is expected except at around 0.4 Å^{-1} if the bundle lattice is modified upon adsorption. Indeed, even for the largest adsorbed amounts, the diffraction pattern recorded after adsorption of ^{40}Ar is virtually indistinguishable from the bare SWNTB spectrum displayed in Fig. 3(a), as revealed in the difference spectrum [dotted line in Fig. 3(b)]. The two spectra reported in Fig. 4(b) for the two highest coverages (0.68 and 2.7 mmol/g) exhibit neither an intensity increase nor a significant peak shift ($\Delta Q \lesssim 0.002$ Å^{-1}). This experiment clearly demonstrates that the maximum shift observed for the largest dose (2.7 mmol/g) of ^{36}Ar results from the diffraction of this isotope and not from an expansion of the bundle lattice. Hence, the overall hexagonal arrangement of the nanotubes into bundles is preserved during the adsorption, with no appreciable modification of its lattice parameter. Note that the coverage increase from 0.68 to 2.7 mmol/g allows the argon molecules to cover the graphene surfaces on the outer surface of the bundles; the energetically favored groove sites and the accessible interstitial channels being already saturated at 0.68 mmol/g (see Fig. 2).

A similar shift of the 0.42 Å^{-1} peak to lower Q values has been observed previously at large coverage by neutron diffraction for CD_4 [3] and O_2 [13] and by x-ray diffraction for O_2 and N_2 [5]. Our results suggest that these apparent dilations are due mainly to the diffraction arising from adsorbates located on the outer part of the surface at a finite binding distance away from the nanotube skeleton, thus forming an expanded envelope around the hexagonal bundle lattice. This, together with the cross interference between the adsorbates and the nanotube lattice gives rise to a shift of the bundle lattice Bragg peaks towards lower Q values [13]. This interpretation is supported by simulations of CD_4 and ^{36}Ar adsorption on SWNTBs. The calculations are carried out using Monte Carlo and molecular dynamics minimization codes [14]. The model takes into account the real atomic structure of the carbon nanotubes and thus allows for any relaxation and deformation of the bundle lattice upon gas adsorption. One of the results is presented in Fig. 4(c) for ^{36}Ar adsorption on a seven (10,10)-nanotube bundle. The calculated set of diffraction patterns around 0.4 Å^{-1} clearly reveals an important peak shift (0.04 Å^{-1}) to lower Q values for the largest coverage. Note that the peak position and width is not the same as the experimental ones because of the limited size of the bundle used for the modeling and the absence of a distribution of nanotube diameters. Also, the maximum peak shift of 0.04 Å^{-1} is larger than the experimental one. This, however, is to be expected if the shift is related to the Ar adsorbed on the outer surface of the bundle, whose relative importance increases with decreasing bundle diameter.

In conclusion, the bundle dilation predicted in Ref. [10] upon adsorption of Ar in the interstitial channels of rigid, monodisperse (10,10) SWNT bundles is not observed in our real sample, in which the nanotubes have a finite diameter distribution. The *apparent* expansion of the bundle lattice parameter as suggested by the shift of the diffraction peak around 0.42 Å^{-1} for higher ^{36}Ar coverages actually results from the diffraction of the atoms located at the *outer* surface of the bundle. The absence of a peak shift to within $\Delta Q \lesssim 0.002$ Å^{-1} for ^{40}Ar doses sets an upper limit for the overall bundle swelling of $\leq 0.5\%$. This value is much smaller than the 2% predicted to be required for stable adsorption into the interstitial channels (IC) in a *homogeneous* bundle [10]. In reality, however, the bundles are not homogeneous and will contain a certain fraction of "wide" ICs which may still be populated by Ar or other species without leading to a sizable *overall* swelling of the bundle [14].

T.W., M. D. P., and O. E. V. acknowledge support from the U.S.A. National Science Foundation through Grant No. DMR 0115663.

*Electronic address: peter.zeppenfeld@jku.at

[1] M. M. Calbi, M.W. Cole, S. M. Gatica, M. J. Bojan, and G. Stan, Rev. Mod. Phys. **73**, 857 (2001).
[2] M. Muris, N. Dufau, M. Bienfait, N. Dupont-Pavlovsky, Y. Grillet, and J.-P. Palmari, Langmuir **16**, 7019 (2000).
[3] M. Muris, M. Bienfait, P. Zeppenfeld, N. Dupont-Pavlovsky, M. Johnson, O. E. Vilches, and T. Wilson, Appl. Phys. A **74**, S1293 (2002).
[4] T. Wilson, A. Tyburski, M. R. DePies, O. E. Vilches, D. Becquet, and M. Bienfait, J. Low Temp. Phys. **126**, 403 (2002).
[5] A. Fujiwara, K. Ishii, H. Suematsu, H. Kataura, Y. Maniwa, S. Suzuki, and Y. Achiba, Chem. Phys. Lett. **336**, 205 (2001).
[6] M. Muris, N. Dupont-Pavlovsky, M. Bienfait, and P. Zeppenfeld, Surf. Sci. **492**, 67 (2001).
[7] S. Talapatra and A. D. Migone, Phys. Rev. Lett. **87**, 206106 (2001).
[8] S. Talapatra and A. D. Migone, Phys. Rev. B **65**, 045416 (2002).
[9] M. S. Dresselhaus, K. A. Williams, and P. C. Eklund, MRS Bull. **24**, 45 (1999).
[10] M. M. Calbi, F. Toigo, and M. W. Cole, Phys. Rev. Lett. **86**, 5062 (2001).
[11] C. Journet, W. K. Maser, P. Bernier, A. Loiseau, M. Lamy de la Chapelle, S. Lefrant, P. Deniard, R. Lee, and J. E. Fisher, Nature (London) **388**, 756 (1997).
[12] S. Rols, R. Almairac, L. Henrard, E. Anglaret, and J. L. Sauvajol, Eur. Phys. J. B **10**, 263 (1999).
[13] M. Bienfait *et al.* (to be published).
[14] M. R. Johnson *et al.*, Chem. Phys. (to be published).